Article

# Electronic Structure and FeNO Conformation of Nonheme Iron–Thiolate–NO Complexes: An Experimental and DFT Study

Jeanet Conradie, Duncan A. Quarless,, Hua-Fen Hsu, Todd C. Harrop, Stephen J. Lippard, Stephen A. Koch, and Abhik Ghosh

*J. Am. Chem. Soc.*, **2007**, 129 (34), 10446-10456• DOI: 10.1021/ja0719982 • Publication Date (Web): 08 August 2007



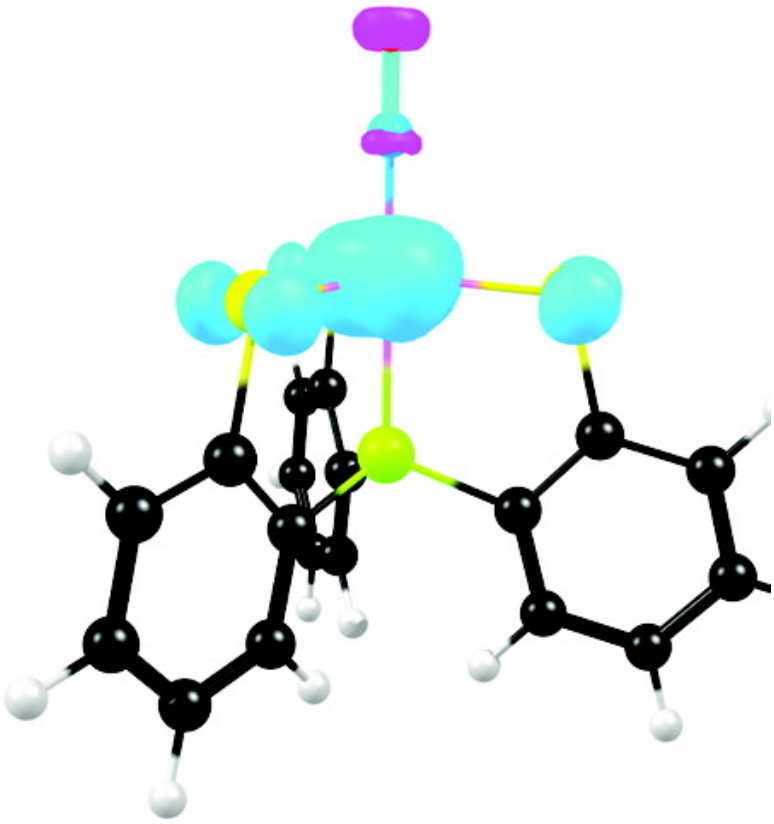

J|A|C|S
ARTICLES
Published on Web 08/08/2007

# Electronic Structure and FeNO Conformation of Nonheme Iron−Thiolate−NO Complexes: An Experimental and DFT Study

Jeanet Conradie,[†,‡] Duncan A. Quarless, Jr.,[§] Hua-Fen Hsu,[§] Todd C. Harrop,[||] Stephen J. Lippard,*[,||] Stephen A. Koch,*[,§] and Abhik Ghosh*[,†]

*Contribution from the Department of Chemistry and Center for Theoretical and Computational Chemistry, University of Tromsø, N-9037 Tromsø, Norway, Department of Chemistry, University of the Free State, 9300 Bloemfontein, Republic of South Africa, Department of Chemistry, State University of New York at Stony Brook, Stony Brook, New York 11794-3400, and Department of Chemistry, Massachusetts Institute of Technology, Cambridge, Massachusetts 02139*

Received March 22, 2007; E-mail: lippard@mit.edu; stephen.koch@sunysb.edu; abhik@chem.uit.no

***Abstract:*** Reactions of NO and CO with Fe(II) complexes of the tripodal trithiolate ligands NS3 and PS3* yield trigonal-bipyramidal (TBP) complexes with varying redox states and reactivity patterns with respect to dissociation of the diatomic ligand. The previously reported four-coordinate $[Fe^{II}(NS3)]^-$ complex reacts irreversibly with NO gas to yield the $S = {}^3/_2$ $\{FeNO\}^7$ $[Fe(NS3)(NO)]^-$ anion, isolated as the $Me_4N^+$ salt. In contrast, the reaction of NO with the species generated by the reaction of $FeCl_2$ with $Li_3PS3^*$ gives a high yield of the neutral, TBP, $S = 1$ complex, [Fe(PS3*)(NO)], the first example of a paramagnetic $\{FeNO\}^6$ complex. X-ray crystallographic analyses show that both $[Fe(NS3)(NO)]^-$ and [Fe(PS3*)(NO)] feature short Fe−N(NO) distances, 1.756(6) and 1.676(3) Å, respectively. However, whereas $[Fe(NS3)(NO)]^-$ exhibits a distinctly bent FeNO angle and a chiral pinwheel conformation of the NS3 ligand, [Fe(PS3*)(NO)] has nearly $C_{3v}$ local symmetry and a linear FeNO unit. The $S = 1$ $[Fe^{II}(PS3)L]$ complexes, where L = 1-MeIm, $CN^-$, CO, and $NO^+$, exhibit a pronounced lengthening of the Fe−P distances along the series, the values being 2.101(2), 2.142(1), 2.165(7), and 2.240(1) Å, respectively. This order correlates with the $\pi$-backbonding ability of the fifth ligand L. The cyclic voltammogram of the $[Fe(NS3)(NO)]^-$ anion shows an irreversible oxidation at +0.394 V (vs SCE), apparently with loss of NO, when scanned anodically in DMF. In contrast, [Fe(PS3*)(NO)] exhibits a reversible $\{FeNO\}^6/\{FeNO\}^7$ couple at a low potential of −0.127 V. Qualitatively consistent with these electrochemical findings, DFT (PW91/STO-TZP) calculations predict a substantially lower gas-phase adiabatic ionization potential for the $[Fe(PS3)(NO)]^-$ anion (2.06 eV) than for $[Fe(NS3)(NO)]^-$ (2.55 eV). The greater instability of the $\{FeNO\}^7$ state with the PS3* ligand results from a stronger antibonding interaction involving the metal $d_{z^2}$ orbital and the phosphine lone pair than the analogous orbital interaction in the NS3 case. The antibonding interaction involving the NS3 amine lone pair affords a relatively "stereochemically active" $d_{z^2}$ electron, the *z* direction being roughly along the Fe−N(NO) vector. As a result, the $\{FeNO\}^7$ unit is substantially bent. By contrast, the lack of a *trans* ligand in $[Fe(S^tBu)_3(NO)]^-$, a rare example of a tetrahedral $\{FeNO\}^7$ complex, results in a "stereochemically inactive" $d_{z^2}$ orbital and an essentially linear FeNO unit.

## Introduction

The biological importance of transition metal−NO interactions provides a powerful impetus for fundamental studies of the coordination chemistry of NO complexes.[1−7] NO is a ubiquitous signaling molecule in eukaryotes[1−4,7] and, as recent studies indicate, in prokaryotes as well.[8] In animals, NO is sensed by the heme protein soluble guanylate cyclase (sGC),[8] where it binds to the Fe(II) center, resulting in a several 100-fold acceleration of the production of cyclic guanosine monophosphate (cGMP) from guanosine triphosphate (GTP). *In vivo*, NO also binds to thiols, Fe(III) porphyrin groups (such as nitrophorin[9] and cytochrome P450 NO reductase[10]), and cys-

[†] University of Tromsø.
[‡] University of the Free State.
[§] State University of New York at Stony Brook.
[||] Massachusetts Institute of Technology.

(1) (a) Murad, F. *Angew. Chem., Int. Ed.* **1999**, *38*, 1856−1868. (b) Furchgott, R. F. *Angew. Chem., Int. Ed.* **1999**, *38*, 1870−1880. (c) Ignarro, L. J. *Angew. Chem., Int. Ed.* **1999**, *38*, 1882−1892.
(2) Gilles-Gonzalez, M. A.; Gonzalez, G. *J. Inorg. Biochem.* **2005**, *99*, 1−22.
(3) *Nitric Oxide: Biology and Pathobiology*; Ignarro, L. J., Ed.; Academic Press: San Diego, CA, 2000; pp 3−19.
(4) Butler, A. R.; Nicholson, R. *Life, Death and Nitric Oxide*; The Royal Society of Chemistry: Cambridge, 2003.
(5) Richter-Addo, G. B.; Legzdins, P. *Metal Nitrosyls*; Oxford University Press: New York, 1992.
(6) (a) McCleverty, J. A. *Chem. Rev.* **2004**, *104*, 403−418. (b) Ford, P. C.; Laverman, L. E. *Coord. Chem. Rev.* **2005**, *249*, 391−403.
(7) Prast, H.; Philippu, A. *Prog. Neurobiol.* **2001**, *64*, 51−68.
(8) Boon, E. M.; Marletta, M. A. *J. Inorg. Biochem.* **2005**, *99*, 892−902.
(9) Weichsel, A.; Maes, E. M.; Andersen, J. F.; Valenzuela, J. G.; Shokhireva, T. K.; Walker, F. A.; Montfort, W. R. *Proc. Natl. Acad. Sci. U.S.A.* **2005**, *102*, 594−599.
(10) Daiber, A.; Shoun, H.; Ullrich, V. *J. Inorg. Biochem.* **2005**, *99*, 185−193.


**10.1021/ja0719982 CCC: $37.00** 

***Scheme 1***

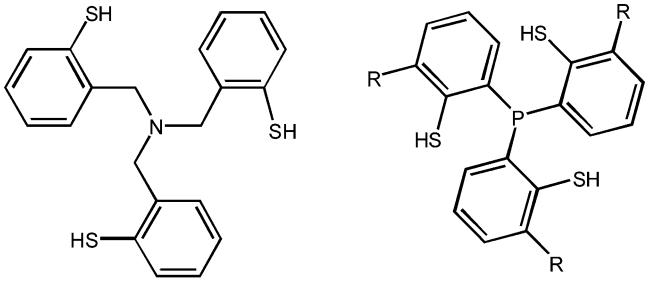


**$H_3NS3$** **$H_3PS3^*$: R = Ph**
**$H_3PS3$: R = H**

teine-ligated nonheme iron.[11] Thus, like RSNO and HNO, cysteine-ligated dinitrosyl iron complexes (DNICs) are believed to act as agents for the storage and transport of NO in biological systems.[12] DNICs have also been implicated in the reduction of NO cytotoxicity[13] and have been suggested as intermediates in the iron-catalyzed degradation and formation of S-nitrosothiols.[14] However, relatively little is known about the mechanistic details of the *in vivo* generation[15] and reactivity of DNICs, which underscores the need for establishing the fundamental chemistry of iron−thiolate−nitrosyl ternary interactions.

Here we present an experimental and density functional theory (DFT) study of the $S = {}^3/_2$ trigonal-bipyramidal (TBP) $\{FeNO\}^7$ complex, $[Fe(NS3)(NO)]^-$, and of the first example of an $S = 1$ $\{FeNO\}^6$ complex, [Fe(PS3*)(NO)] (see Scheme 1).[16] Elsewhere we have also reported the synthesis and full characterization of the $S = 1$ $[Fe^{II}(PS3^*)(CO)]^-$ and $[Fe^{II}(PS3)(CN)]^{2-}$ anions.[17a,34] In addition, using DFT calculations, we compare the bonding in these TBP complexes with that in the recently reported, pseudotetrahedral $\{FeNO\}^7$ anion, $[Fe(S^tBu)_3(NO)]^-$.[18] The combined experimental and DFT approach has afforded substantial insights into the electronic structure and conformational properties of nonheme iron−nitrosyl complexes.

## Results and Discussion

**Synthesis of NS3 and PS3* Complexes.** Reactions of NO and CO with Fe(II) complexes of the tripodal trithiolate ligands NS3 and PS3* (Scheme 1) yield TBP complexes with varying redox states and reactivity patterns with respect to dissociation of the diatomic ligand. $[Me_4N][Fe(NS3)(NO)]$ (**1**) is prepared by the reaction of the previously reported four-coordinate $[Fe^{II}(NS3)]^-$ complex[19] with NO gas. The NO binding reaction is essentially irreversible; the coordinated NO does not dissociate at room temperature. The observed $\{FeNO\}^7$ redox level is as anticipated for the reaction of an Fe(II) complex with NO. In contrast, the reaction of NO with the presumptive $Fe^{II}$ complex generated by the addition of $FeCl_2$ with $Li_3PS3^*$ gives a high yield of the neutral $\{FeNO\}^6$ complex [Fe(PS3*)(NO)] (**2**), presumably via an oxidative nitrosylation reaction. Under similar conditions, the analogous reaction with CO proceeds without oxidation to give the previously reported $[Et_4N][Fe^{II}(PS3^*)(CO)]$.[17a] For the [Fe(PS3*)] system, a four-coordinate complex is unknown and the NO and CO ligands in the PS3* complexes do not dissociate even at elevated temperatures. In contrast to the tight binding of CO in $[Fe(PS3^*)(CO)]^-$, CO binds reversibly to $[Fe^{II}(NS3)]^-$ and, therefore, the synthesis, recrystallization, and spectroscopic studies of $[(n\text{-}C_5H_{11})_4N][Fe(NS3)(CO)]$ must be carried out under a CO atmosphere.[20] With regard to the dissociation of CO and NO, the $[Fe(NS3)(XO)]^-$ complexes appear to resemble the similar TBP complexes with triamidoamine ligands[21−23] and the tris(ethylthiolato)amine ligand.[24,25]

**Structures of $[Fe(NS3)(NO)]^-$ and [Fe(PS3*)(NO)].** The X-ray crystal structure of $[Me_4N][Fe(NS3)(NO)]\cdot CH_3OH$ (Figure 1) revealed it to be a TBP $\{FeNO\}^7$ compound with a bent FeNO group disrupting the approximate threefold symmetry (Table 1). The FeNO group is twofold-disordered with Fe−N−O angles of 146(2)° and 148(2)°. The chiral pinwheel conformation of the NS3 ligand is a common feature of this tetradentate ligand, when coordinated. A $C_3$ conformation has previously been observed for $[Ga^{III}(NS3)]$, $[Fe^{II}(NS3)]^-$, and related complexes of Co(II), Ni(II), Zn(II), Cd(II), and Hg(II), as well as for $[M^{III}(NS3)(1\text{-MeIm})]$ (M = Ga, Fe and In) and $[In^{III}(NS3)(DMF)]$.[19,26,27]

A comparison of the structure of **1** with that of $[Fe^{II}(NS3)]^-$ reveals the geometric changes associated with NO binding

(11) Szacilowski, K.; Chmura, A.; Stasicka, Z. *Coord. Chem. Rev.* **2005**, *249*, 2408−2436.
(12) (a) Alencar, J. L.; Chalupsky, K.; Sarr, M.; Schini-Kerth, V.; Vanin, A. F.; Stoclet, J.-C.; Muller, B. *Biochem. Pharmacol.* **2003**, *66*, 2365−2374. (b) Wiegant, F. A. C.; Malyshev, I. Y.; Kleschyov, A. L.; van Faassen, E.; Vanin, A. F. *FEBS Lett.* **1999**, *455*, 179−182. (c) Vanin, A. F.; Stukan, R. A.; Manukhina, E. B. *Biochim. Biophys. Acta* **1996**, *1295*, 5−12.
(13) Kim, Y.-M.; Chung, H.-T.; Simmons, R. L.; Billiar, T. R. *J. Biol. Chem.* **2000**, *275*, 10954−10961.
(14) (a) Costanzo, S.; Menage, S.; Purrello, R.; Bonomo, R. P.; Fontecave, M. *Inorg. Chim. Acta* **2001**, *318*, 1−7. (b) Vanin, A. F. *Biochem.* (*Moscow*) **1998**, *63*, 782−793.
(15) (a) Yang, W.; Rogers, P. A.; Ding, H. *J. Biol. Chem.* **2002**, *277*, 12868−12873. (b) Cruz-Ramos, H.; Crack, J.; Wu, G.; Hughes, M. N.; Scott, C.; Thomson, A. J.; Green, J.; Poole, R. K. *EMBO J.* **2002**, *21*, 3235−3244. (c) Foster, M. W.; Cowan, J. A. *J. Am. Chem. Soc.* **1999**, *121*, 4093−4100.
(16) The superscripts 6 and 7 refer to Enemark−Feltham electron counts, defined as the sum of the numbers of metal d and NO $\pi^*$ electrons: Westcott, B. L.; Enemark, J. H. In *Inorganic Electronic Structure and Spectroscopy*; Solomon, E. I., Lever, A. B. P., Eds.; Wiley: New York, 1999; Vol. 2, pp 403−450.
(17) (a) Nguyen, D. H.; Hsu, H.-F.; Millar, M.; Koch, S. A.; Achim, C.; Bominaar, E. L.; Münck, E. *J. Am. Chem. Soc.* **1996**, *118*, 8963−8964. (b) Franolic, J. D.; Wang, W. Y.; Millar, M. *J. Am. Chem. Soc.* **1992**, *114*, 6588−6589.
(18) Harrop, T. C.; Song, D.; Lippard, S. J. *J. Am. Chem. Soc.* **2006**, *128*, 3528−3529.
(19) Govindaswamy, N.; Quarless, D. A., Jr.; Koch, S. A. *J. Am. Chem. Soc.* **1995**, *117*, 8468−9.
(20) Because of the instability of $[(n\text{-}C_5H_{11})_4N][Fe(NS3)(CO)]$, except under a CO atmosphere, this compound was only incompletely characterized. Some experimental details are as follows. Preparation: 10 mL of an ethanol solution of $FeCl_2\cdot 4H_2O$ (0.199 g, 1.00 mmol) and $[(n\text{-}C_5H_{11})_4N]Br$ (3.78 g, 1.00 mmol) were added 5 mL of an ethanol solution of 1.10 mmol of $Li_3(N(CH_2\text{-}o\text{-}C_6H_4S)_3)$. A pale brown precipitate, which formed immediately, redissolved upon the addition of a steady stream of CO to generate a green solution. A crystalline emerald green solid formed and was filtered and dried under a CO atmosphere. Yield: 0.56 g (73 %). IR (Nujol): $\nu_{CO} = 1939$ cm$^{-1}$. X-ray analysis: The compound was recrystallized from DMF/EtOH under a CO atmosphere. An emerald-green trigonal prism (0.34 mm × 0.34 mm × 0.14 mm) was immersed in oil and was cemented inside a capillary with epoxy. A unit cell was determined indicating a trigonal system, space group $P31c$ ($a = b = 18.261(2)$ Å, $c = 17.722(4)$ Å, $V = 5117.7(1)$ Å$^3$, $Z = 6$). The collected data set was not sufficient for structural analysis.
(21) Ray, M.; Golombek, A. P.; Hendrich, M. P.; Young, V. G., Jr.; Borovik, A. S. *J. Am. Chem. Soc.* **1996**, *118*, 6084−6085.
(22) Hammes, B. S.; Ramos-Maldonado, D.; Yap, G. P. A.; Liable-Sands, L.; Rheingold, A. L.; Young, V. G. Jr.; Borovik, A. S. *Inorg. Chem.* **1997**, *36*, 3210−3211.
(23) Ray, M.; Golombek, A. P.; Hendrich, M. P.; Yap, G. P. A.; Liable-Sands, L. M.; Rheingold, A. L.; Borovik, A. S. *Inorg. Chem.* **1999**, *38*, 3110−3115.
(24) Davies, S. C.; Durrant, M. C.; Hughes, D. L.; Richards, R. L.; Sanders, J. R. *J. Chem. Soc., Dalton Trans.* **2000**, 4694−4701.
(25) Davies, S. C.; Evans, D. J.; Hughes, D. L.; Konkol, M.; Richards, R. L.; Sanders, J. R.; Sobota, P. *J. Chem. Soc., Dalton Trans.* **2002**, 2473−2482.
(26) Motekaitis, R. J.; Martell, A. E.; Koch, S. A.; Hwang, J. W.; Quarless, D. A., Jr.; Welch, M. J. *Inorg. Chem.* **1998**, *37*, 5902−5911.
(27) Quarless, D. A.; Hsu, H.-F.; Koch, S. A. Unpublished results.

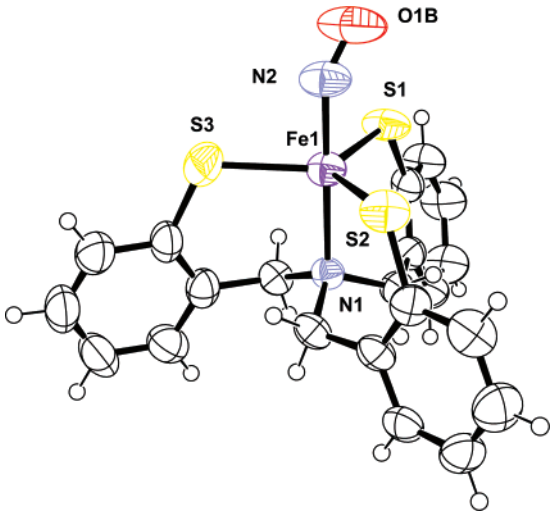


***Figure 1.*** X-ray crystal structure of the anion of $[Me_4N][Fe(NS3)(NO)]$ (**1**). See Table 1 for metrical parameters.

***Table 1.*** Selected Bond Distances (Å) and Angles (deg) for $[Me_4N][Fe(NS3)(NO)]$ (**1**)[a]

| | | | |
|---|---|---|---|
| Fe1−N1 | 2.178(4) | S2−Fe1−S3 | 119.33(7) |
| Fe1−N2 | 1.756(6) | N1−Fe1−N2 | 176.3(2) |
| Fe1−S1 | 2.3064(17) | N1−Fe1−S1 | 92.07(11) |
| Fe1−S3 | 2.3207(19) | N1−Fe1−S2 | 91.61(12) |
| Fe1−S2 | 2.3493(18) | N1−Fe1−S3 | 91.91(12) |
| N2−O1B | 1.11(3) | N2−Fe1−S1 | 84.70(18) |
| N2−O1A | 1.18(2) | N2−Fe1−S2 | 91.71(19) |
| Fe1−N2−O1A | 145.9(16) | N2−Fe1−S3 | 87.9(2) |
| Fe1−N2−O1B | 147.8(19) | Fe1−S1−C7 | 114.7(2) |
| S1−Fe1−S2 | 122.80(7) | Fe1−S2−C14 | 113.8(2) |
| S1−Fe1−S3 | 117.55(8) | Fe1−S3−C21 | 113.8(2) |

[a] See Figure 1 for atom labeling scheme.

(Table 2). The $[Fe^{II}(NS3)]^-$ anion exhibits a pseudotetrahedral geometry with the Fe atom 0.37 Å below the plane of the three S atoms, an $Fe-N_{amine}$ distance of 2.127(5) Å, and an $Fe-S_{av}$ distance of 2.314(13) Å.[19] NO coordination results in a lengthening of the $Fe-N_{amine}$ bond (2.178(4) Å), only a small change in $Fe-S_{av}$ distance, and the movement of the Fe atom toward, but still 0.08 Å "below", the $S_3$ plane. The three $N_{amine}-Fe-S$ angles are nearly equal and slightly greater than 90°: 92.07(11)°, 91.61(12)°, 91.91(12)°; as a result, the average S−Fe−N(O) angle is 88.1°. This acute $L_{equatorial}-M-N(O)$ average angle is unusual; normally, the strong bonds involving diatomics such as CO and NO result in $L_{equatorial}-M-X(O)$ angles that exceed 90°. The structure of the NS3 ligand results in complexes with six-membered metal-chelate rings and an observed tendency to disfavor coordination of a fifth ligand for first row transition elements in the $M^{2+}$ oxidation state.[19,27] Although we were unable to get an X-ray structure of $[Fe^{II}(NS3)(CO)]^-$, it is likely that it would also feature the unusual acute $L_{equatorial}-M-C(O)$ angles. This property may well contribute to the lability of the CO ligand in this complex.

In $\{FeNO\}^7$ porphyrin complexes, it has often been observed that the Fe−N(O) bond is tilted away from the normal to the porphyrin ring system and in the direction of the bending of the FeNO group.[28−30] A similar but smaller tilt of the Fe−N(O) bond is observed for **1**; the Fe−N(O) vector tilts by 4° from the normal to the $S_3$ plane and in the direction of the Fe−S1 bond. The distortion results from the off-axis tilting of the Fe−N(O) bond rather than a distortion of the FeNS3 unit. Although the tilt is small, it does result in the S1−Fe−N(O) angle of 84.7(2)° being less than the S2−Fe−N(O) (91.7(2)°) and S3−Fe−N(O) (87.9(2)°) angles. The Fe−S1 bond is shorter than Fe−S2 and Fe−S3. As discussed in greater detail below, the strong cooperativity of tilting and bending distortions was first noted over a decade ago[31] and later explained in molecular orbital terms.[32,33]

Compound **1** is structurally analogous to $[Fe(N(CH_2CH_2S)_3)NO)]^-$, which also has the $\{FeNO\}^7$ electronic configuration,[25] in terms of similar Fe−N(O) distances, Fe−N−O angles, and Fe−S distances (see Table 2). The smaller five-membered metal-chelate rings in $[Fe(N(CH_2CH_2S)_3)(NO)]^-$, however, result in the Fe atom being 0.35 Å above the plane of the three S atoms in the direction of the NO ($S-Fe-N(O)_{ave}$ 95°). When discussing the electronic structures of the various complexes, we will see that it is useful to view the $[Fe(NS3)(NO)]^-$ and $[Fe(N(CH_2CH_2S)_3)(NO)]^-$ complexes as models of the hypothetical product of the addition of a ligand trans to NO in the $[Fe(S^tBu)_3(NO)]^-$ complex.[18]

[Fe(PS3*)(NO)] (**2**) has a TBP structure with the P atom and the linear NO ligand on the pseudo-threefold axis (Figure 2). The near-linear Fe−N−O angle of 175.2(3)° in this $\{FeNO\}^6$ compound is associated with a very short Fe−N distance of 1.676(3) Å (Table 3). A series of five- and six-coordinate compounds, $[Fe^{II,III}(PS3)L]$ (L = CO, $CN^-$, 1-MeIm) and $[Fe^{II,III}(PS3)L_2]$ ($L_2$ = $(CN)_2$, $(CO)_2$, and (CO)(CN)), were characterized in the course of earlier studies.[17a,27,34] [Fe(PS3*)(NO)] is the third structurally characterized member of an isoelectronic series that includes $[Fe^{II}(PS3*)(CO)]^-$ and $[Fe^{II}(PS3)(CN)]^{2-}$.[17a,34] Each of these three compounds has an $S = 1$ ground state; the TBP stereochemistry does not allow a diamagnetic ($S = 0$) ground state for $d^6$ (Fe(II)) or $\{FeNO\}^6$ complexes. Although there are many examples of $\{FeNO\}^6$ complexes,[35,36] [Fe(PS3*)(NO)] is the first example of a trigonal-bipyramidal $\{FeNO\}^6$ complex as well as of a paramagnetic $\{FeNO\}^6$ species. The $[Fe(PS3*)(CO)]^-$ complex is also a rare example of a paramagnetic $d^6$ metal carbonyl.[17a,21,24]

The PS3 (or PS3*) ligand has a stronger effective ligand field than the NS3 ligand. Thus, $[Fe^{III}(NS3)(1\text{-MeIm})]$ is high-spin

(28) Scheidt, W. R.; Duval, H. F.; Neal, T. J.; Ellison, M. K. *J. Am. Chem. Soc.* **2000**, *122*, 4651−4659.
(29) Wyllie, G. R. A.; Scheidt, W. R. *Chem. Rev.* **2002**, *102*, 1067−1089.
(30) Ghosh, A.; Wondimagegn, T. *J. Am. Chem. Soc.* **2000**, *122*, 8101−8102.
(31) Ghosh, A.; Bocian, D. F. *J. Phys. Chem.* **1996**, *100*, 6363−6367.
(32) Papai, I.; Stirling, A.; Mink, J.; Nakamoto, K. *Chem. Phys. Lett.* **1998**, *287*, 531−534.
(33) Ghosh, A. *Acc. Chem. Res.* **2005**, *38*, 943−954.
(34) Hsu, H.-F.; Koch, S. A.; Popescu, C. V.; Münck, E. *J. Am. Chem. Soc.* **1997**, *119*, 8371−8372.
(35) Joseph, C. A.; Lee, M. S.; Iretskii, A. V.; Wu, G.; Ford, P. C. *Inorg. Chem.* **2006**, *45*, 2075−2082.
(36) (a) Schweitzer, D.; Ellison, J. J.; Shoner, S. C.; Lovell, S.; Kovacs, J. A. *J. Am. Chem. Soc.* **1998**, *120*, 10996−10997. (b) Hauser, C.; Glaser, T.; Bill, E.; Weyhermuller, T.; Wieghardt, K. *J. Am. Chem. Soc.* **2000**, *122*, 4352−4365. (c) Li, M.; Bonnet, D.; Bill, E.; Neese, F.; Weyhermuller, T.; Blum, N.; Sellman, D.; Wieghardt, K. *Inorg. Chem.* **2002**, *41*, 3444−3456. (d) Serres, R. G.; Grapperhaus, C. A.; Bothe, E.; Bill, E.; Weyhermuller, T.; Neese, F.; Wieghardt, K. *J. Am. Chem. Soc.* **2004**, *126*, 5138−5153. (e) Afshar, R. K.; Patra, A. K.; Bill, E.; Olmstead, M. M.; Mascharak, P. K. *Inorg. Chem.* **2006**, *45*, 3774−3781. (f) Harrop, T. C.; Olmstead, M. M.; Mascharak, P. K. *Inorg. Chem.* **2005**, *44*, 6918−6920. (g) Patra, A. K.; Rose, M. J.; Olmstead, M. M.; Mascharak, P. K. *J. Am. Chem. Soc.* **2004**, *126*, 4780−4781. (h) Afshar, R. K.; Patra, A. K.; Olmstead, M. M.; Mascharak, P. K. *Inorg. Chem.* **2004**, *43*, 5736−5743. (i) Patra, A. K.; Rowland, J. M.; Marlin, D. S.; Bill, E.; Olmstead, M. M.; Mascharak, P. K. *Inorg. Chem.* **2003**, *42*, 6812−6823. (j) Lopez, J. P.; Heinemann, F. W.; Prakash, R.; Hess, B. A.; Horner, O.; Jeandey, C.; Oddou, J.-L.; Latour, J.-M.; Grohmann, A. *Chem.−Eur. J.* **2002**, *8*, 5709−5722. (k) Gonzalez Lebrero, M. C.; Scherlis, D. A.; Estiu, G. L.; Olabe, J. A.; Estrin, D. A. *Inorg. Chem.* **2001**, *40*, 4127−4133.

***Table 2.*** Bond Distances (Å) for Fe Complexes with Tripodal Trithiolate Ligands and Other Related Compounds

| compound | Fe–S | Fe–N/P | Fe–XO | $\nu_{XO}$ ($cm^{-1}$) | ref |
|---|---|---|---|---|---|
| $[Me_4N][Fe(NS3)(NO)]$ (**1**) | 2.325(20) | 2.178(4) | 1.756(6) | 1639 | this work |
| $[Ph_4P][Fe^{II}(NS3)]$ | 2.314(13) | 2.127(5) | | | 19 |
| $[(n\text{-}C_5H_{11})_4N][Fe^{II}(NS3)(CO)]$ | na | na | na | 1939 | this work |
| $[Fe^{III}(NS3)(1\text{-MeIm})]$ | 2.302(6) | 2.21(1) | 2.15(1) | | 19 |
| [Fe(PS3*)(NO)] (**2**) | 2.242(3) | 2.240(1) | 1.676(3) | 1807 | this work |
| $[Et_4N][Fe^{II}(PS3^*)(CO)]$ | 2.290(4) | 2.165(7) | 1.88(3) | 1940 | 17a |
| $[Me_3BzN]_2[Fe^{II}(PS3)(CN)]$ | 2.29(2) | 2.142(1) | Fe−C(N) 1.947(4) | 2070 (CN) | 34 |
| $[(n\text{-}Bu)_4N][Fe^{II}(PS3)(1\text{-MeIm})]$ | 2.280(8) | 2.101(2) | 2.029(6) | | 27 |
| $Li(DMF)_3[Fe^{III}(PS3)(CN)]$ | 2.167(1) | 2.141(2) | Fe−C(N) 1.938(7) | 2094 (CN) | 34 |
| $[Fe^{III}(PS3)(1\text{-MeIm})]$ | 2.179(2) | 2.1322(12) | 2.016(3) | | 27 |
| $[Et_4N][Fe(N(CH_2CH_2S)_3)(CO)]$ | 2.276 | 2.035(7) | 1.716(11) | 1910 | 22 |
| $[Et_4N][Fe(N(CH_2CH_2S)_3(NO)]$ | 2.314 | 2.232(7) | 1.721(8) | 1621 | 25 |
| $K[Fe(N(CH_2CONPr^i)_3)(NO)]$ | | 2.189(3) | 1.737(4) | 1729 | 23 |
| $K[Fe^{II}(N(CH_2CONPr^i)_3)(CO)]$ | | 1.991(3) | 1.749(3) | 1940 | 21 |
| $[Et_4N][Fe(S^tBu)_3(NO)]$ | 2.2737(4) | | 1.7110(14) | 1704 | 18 |

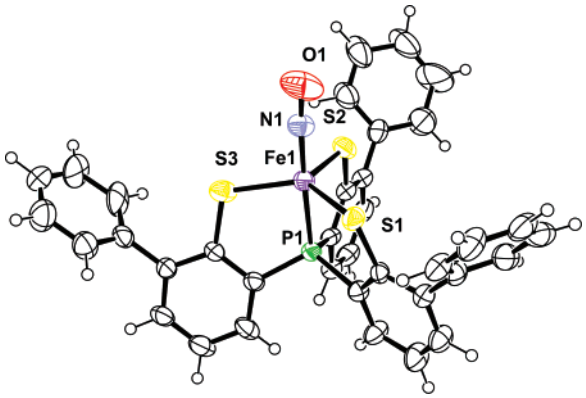


***Figure 2.*** X-ray crystal structure of [Fe(PS3*)(NO)] (**2**). See Table 3 for metrical parameters.

***Table 3.*** Selected Bond Distances (Å) and Angles (deg) for [Fe(PS3*)(NO)] (**2**)[a]

| | | | |
|---|---|---|---|
| Fe1−S1 | 2.245(1) | S2−Fe1−S3 | 115.56(5) |
| Fe1−S2 | 2.239(1) | S1−Fe1−P1 | 84.35(4) |
| Fe1−S3 | 2.247(1) | S2−Fe1−P1 | 86.35(5) |
| Fe1−P1 | 2.240(1) | S3−Fe1−P1 | 84.53(4) |
| Fe1−N1 | 1.676(3) | S1−Fe1−N1 | 94.59(12) |
| N1−O1 | 1.154(5) | S2−Fe1−N1 | 92.27(12) |
| Fe1−N1−O1 | 175.2(3) | S3−Fe1−N1 | 97.71(12) |
| P1−Fe1−N1 | 177.72(12) | Fe1−S1−C2 | 108.69(13) |
| S1−Fe1−S2 | 114.62(5) | Fe1−S2−C14 | 107.63(13) |
| S1−Fe1−S3 | 127.55(5) | Fe1−S3−C26 | 108.53(13) |

[a] See Figure 2 for atom labeling scheme.

($S = {}^5/_2$) with Fe−$S_{av}$ 2.302(6) Å and Fe−$N_{amine}$ 2.21(1) Å,[19] whereas $[Fe^{III}(PS3)(1\text{-MeIm})]$ is low-spin ($S = {}^1/_2$) with Fe−$S_{ave}$ 2.179(2) Å and Fe−P 2.1322(12) Å.[27] Similarly, $[Fe^{II}(PS3)(1\text{-MeIm})]^-$ has a low-spin ($S = 1$) ground state,[27] whereas $S = 2$ $[Fe^{II}(NS3)]^-$ does not coordinate 1-MeIm.[19] The PS3 ligand differs from the NS3 ligand not only in the identity of the P and N donors but also in forming five- rather than six-membered metal-chelate rings. In all [Fe(PS3)L] complexes, the smaller chelate ring size results in a displacement of the Fe atom above the $S_3$ equatorial plane toward the fifth ligand. Thus, for [Fe(PS3*)(NO)], the average S−Fe−N(O) angle is 94.9°. The NS3 and the $(N(CH_2CH_2S)_3)$ ligands appear to be comparable in their effective ligand field.[24,25]

The phenyl-substituted PS3* ligand was introduced by Millar[17a] to help control the tendency of metal complexes of the unsubstituted PS3 ligand to dimerize to form $[M_2(PS3)_2]^{n-}$ (M = Ni, Fe, and Co) complexes.[17b] We initially used the PS3* ligand for the synthesis of monomeric Fe complexes; however, subsequent work showed that PS3* and PS3 could be employed interchangeably to access $[Fe^{II,III}(PS3)L]$ compounds.[34] Accordingly, we have substituted the simpler PS3 ligand for PS3* in our computational studies (*vide infra*).

The $[Fe^{II}(PS3/PS3^*)L]$ series of complexes (Table 2), where L = 1-MeIm, $CN^-$, and CO, display a systematic increase in the Fe−P distances, from 2.101(2) to 2.142(1) to 2.165(7) Å, which correlates with the $\pi$-backbonding ability of the fifth ligand L; there are only small changes in the Fe−$S_{av}$ distances across the series. For [Fe(PS3*)(NO)], there is a large increase in the Fe−P distance (2.240(1) Å) and a dramatic decrease in the Fe−$S_{av}$ distance (2.242(3) Å). This type of structural *trans* influence is not seen in octahedral {FeNO}$^6$ porphyrin complexes. Instead, there is a decrease in the Fe−N(1-MeIm) distance in [Fe(OEP)(1-MeIm)(XO)] on going from CO (2.077(3) Å)[37] to {FeNO}$^6$ NO (1.989(2) Å).[38] Similar effects are also observed in six-coordinate nonheme compounds.[36] Although we have not examined this point in detail, a simple explanation for the shortening of the Fe−S bond distance in **2** is the contribution of the $Fe^{III}(NO)$ vs $Fe^{II}(NO^+)$ resonance structures. The Fe−S bonds in **2** are, however, considerably longer than those in low-spin ($S = {}^1/_2$) $[Fe^{III}(PS3)L]$ complexes where L is a relatively innocent ligand. Examples include $[Fe^{III}(PS3)(CN)]^-$ (Fe−S 2.167(1) Å, Fe−P 2.141(2) Å) and $[Fe^{III}(PS3)(1\text{-MeIm})]$ (Fe−S 2.179(2) Å, Fe−P 2.1322(12) Å).[34,27]

**Vibrational Spectroscopy.** For $C_3$-symmetric TBP $S = 1$ $Fe^{II}CO$ complexes, there is no direct relationship between the CO stretching frequency and the lability of the bound CO ligand. For example, $[Et_4N][Fe^{II}(PS3^*)(CO)]$ ($\nu_{CO}$ 1940 $cm^{-1}$), $[(n\text{-}C_5H_{11})_4N][Fe^{II}(NS3)(CO)]$ (1939 $cm^{-1}$), and $K[Fe^{II}(N(CH_2CONPr^i)_3)(CO)]$ (1940 $cm^{-1}$)[21] have virtually identical CO stretching frequencies, although the last two compounds are only stable in solution under a CO atmosphere whereas the first compound does not release CO under continuous vacuum, in solution, or in the solid state. The CO ligand in $[Et_4N][Fe^{II}(N(CH_2CH_2S)_3)(CO)]$ (1910 $cm^{-1}$) exchanges with $^{13}CO$.[39] Thus, there

(37) Salzmann, R.; McMahon, M. T.; Godbout, N.; Sanders, L. K.; Wojdelski, M.; Oldfield, E. *J. Am. Chem. Soc.* **1999**, *121*, 3818−3828.
(38) Ellison, M. K.; Scheidt, W. R. *J. Am. Chem. Soc.* **1999**, *121*, 5210−5219.
(39) Smith, M. C.; Barclay, J. E.; Cramer, S. P.; Davies, S. C.; Gu, W.-W.; Hughes, D. L.; Longhurst, S.; Evans, D. J. *J. Chem. Soc., Dalton Trans.* **2002**, 2641−2647.

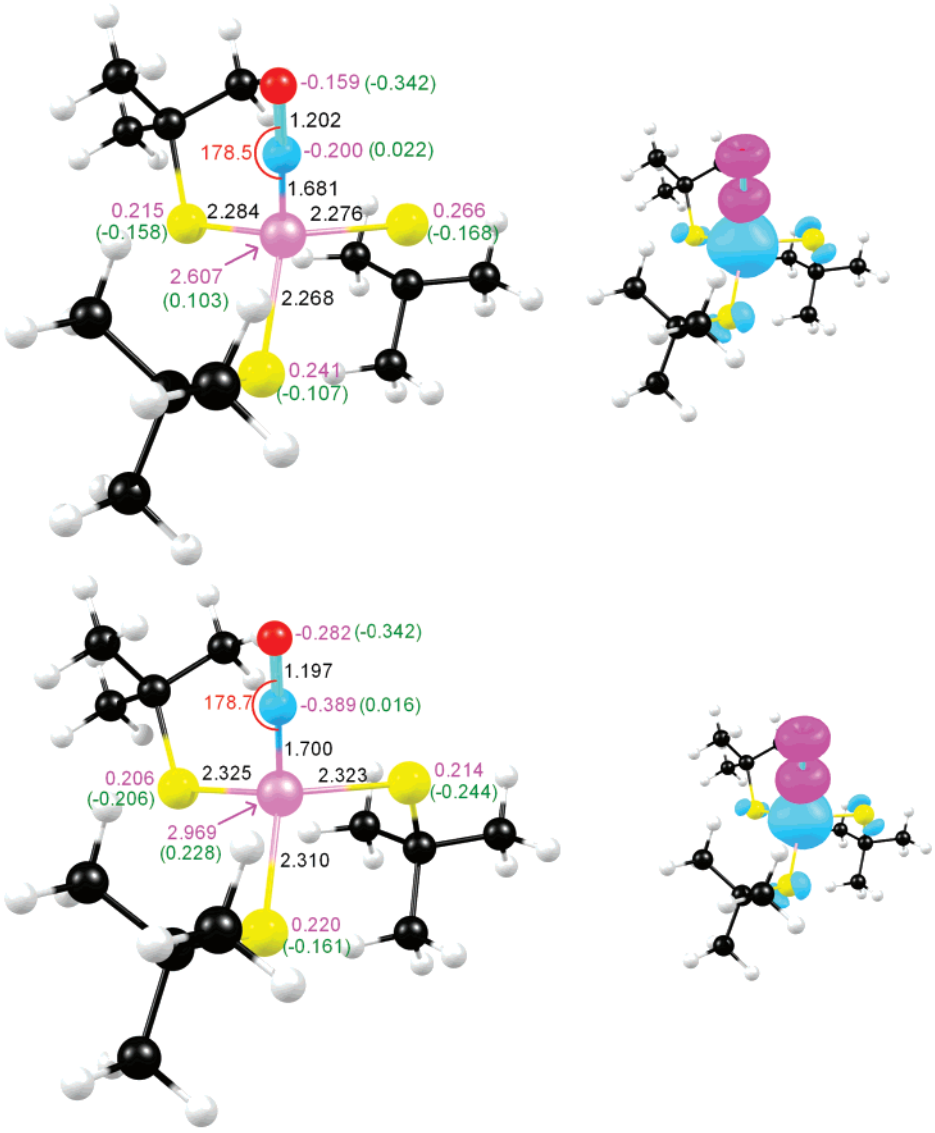


***Figure 3.*** Selected PW91 (top) and OLYP (bottom) results for $[Fe(S^tBu)_3(NO)]^-$. Highlights of optimized distances (Å, in black) and angles (deg, in red), Mulliken charges (in green), and Mulliken spin populations (in magenta) are shown in the left-hand graphics. Shown to the right are molecular spin density profiles, where majority and minority spin densities are indicated in cyan and magenta, respectively. Color code for atoms in Figures 3−7: C (black), H (ivory), N (cyan), O (red), S (yellow), and P (lime-green).

is no simple correlation between CO stretching frequency and the position of the Fe(L) + CO = Fe(L)(CO) equilibrium.

Understanding trends in NO stretching frequencies of Fe nitrosyl complexes is not straightforward either. The observed ranges of NO stretching frequencies for $\{FeNO\}^6$ and $\{FeNO\}^7$ compounds are well established and often correlate with the redox state. For $\{FeNO\}^6$ compounds, the NO stretching frequencies span a wide range, from 1760 to 1940 $cm^{-1}$, but there is no correlation between the Fe−N(O) distance and $\nu_{NO}$. The situation for $\{FeNO\}^6$ porphyrin complexes has been discussed in detail.[40]

**Electrochemistry.** Both members of the $\{FeNO\}^6/\{FeNO\}^7$ couple have never been fully characterized for any TBP FeNO complex. The $[Fe(NS3)(NO)]^-$ anion undergoes an irreversible oxidation at +0.394 V (vs SCE) when scanned anodically in DMF. This oxidation is apparently accompanied by loss of NO from the complex because the reduction during the reverse scan is observed at −0.128 V, which is the $E_{1/2}$ value for the $Fe^{3+}/Fe^{2+}$ couple of $[Ph_4P][Fe^{II}(NS3)]$.[19] The $[Fe(N(CH_2CONPr^i)_3)(NO)]^-$ anion undergoes a reversible oxidation at 0.56 V (vs SCE), but the $\{FeNO\}^6$ complex produced via controlled potential electrolysis decays within minutes.[23] In contrast, the cyclic voltammogram of **2** exhibits a reversible $\{FeNO\}^6/\{FeNO\}^7$ couple at a potential of −0.127 V (vs SCE), similar to that of a related complex.[36f] The $\{FeNO\}^7$ PS3* species can also be generated electrochemically by controlled potential electrolysis. However, attempts to reduce **2** chemically and isolate the $\{FeNO\}^7$ species have not been successful. The $[Fe(PS3^*)(CO)]^-$ anion displays a reversible oxidation at +0.083 V (vs SCE); however, bulk electrolysis indicates that the oxidation is associated with loss of CO. Electrochemical studies of $[Fe(N(CH_2CH_2S)_3)(CO)]^-$ and $[Fe(N(CH_2CH_2S)_3)(NO)]^-$ have not been reported.

**Comparative Theoretical Description of $[Fe(S^tBu)_3(NO)]^-$ and $[Fe(NS3)(NO)]^-$.** Compared with metalloporphyrin−NO

(40) (a) Linder, D. P.; Rodgers, K. R.; Banister, J.; Wyllie, G. R. A.; Ellison, M. K.; Scheidt, W. R. *J. Am. Chem. Soc.* **2004**, *126*, 14136−14148. (b) Linder, D. P.; Rodgers, K. R. *Inorg. Chem.* **2005**, *44*, 1367−1380.

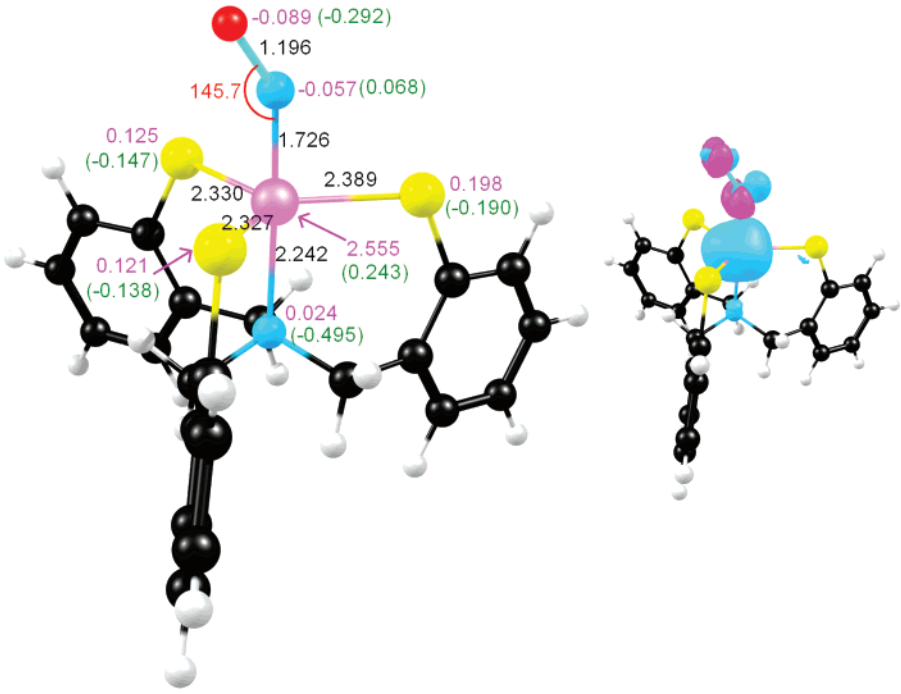


***Figure 4.*** Selected PW91/TZP results for $[Fe(NS3)(NO)]^-$ ($S = {}^3/_2$). Left: Distances (Å, in black), angles (deg, in red), Mulliken charges (in green), and spin populations (in magenta). Right: A molecular spin density plot; majority and minority spin densities are indicated in cyan and magenta, respectively.

***Table 4.*** Comparison of PW91 and Experimental (in Parentheses) Geometry Parameters (Å, deg) for Selected FeNO Complexes

| species | *S* | Fe–X(Y) | X–Y | Fe–S (av) | Fe–$L_{trans}$ | ∠FeXY |
|---|---|---|---|---|---|---|
| $[Fe(S^tBu)_3(NO)]^-$ | $^3/_2$ | 1.681 | 1.202 | 2.276 | – | 178.5 |
| | | (1.711) | (1.168) | (2.273) | | (174.2) |
| $[Fe(NS3)(NO)]^-$ | $^3/_2$ | 1.725 | 1.197 | 2.315 | 2.242 | 145.7 |
| | | (1.756) | (1.11, 1.18)[a] | (2.325) | (2.178) | (145.9, 147.8)[a] |
| [Fe(PS3)(NO)][b] | 1 | 1.667 | 1.171 | 2.250 | 2.261 | 180.0 |
| | | (1.676) | (1.153) | (2.242) | (2.240) | (175.1) |

[a] Disordered NO. [b]The experimental results within parentheses are for [Fe(PS3*)(NO)].

complexes,[33] nonheme NO complexes have been relatively little explored by means of theoretical calculations.[36c,d,j,k,41] In principle, nearly all aspects of the NO complexes reported here lend themselves to fruitful quantum chemical explorations. However, to circumscribe the scope of the present study, we chose to limit our theoretical studies to two principal themes, namely, the degree of FeNO bending in nonheme NO complexes and the relative stabilities of the $\{FeNO\}^7$ versus $\{FeNO\}^6$ states.

Figure 3 depicts selected calculated results for $[Fe(S^tBu)_3(NO)]^-$, including highlights of the symmetry-unconstrained optimized geometry for the PW91 and OLYP functionals,[42,43] Mulliken charges, and spin populations, as well as spin density plots. Figure 4 presents the corresponding information for the $[Fe(NS3)(NO)]^-$ anion. In addition, Table 4 compares key calculated and experimental geometry parameters for the FeNO complexes studied. The results raise a number of points that merit discussion.

In general, the PW91 geometries are in reasonably good agreement with experiment. The calculated NO distances are about 0.02−0.03 Å longer than those observed in the X-ray crystal structures, however, which may be viewed as a small systematic error. The only other substantial error in the PW91 geometries is in the Fe−N(NS3) distance in $[Fe(NS3)(NO)]^-$, where theory (2.242 Å) exceeds experiment (2.178 Å) by about 0.06 Å. Such errors have been documented for relatively weak bonds that are *trans* to much shorter and stronger metal−ligand bonds, e.g., in six-coordinate iron-nitro porphyrins.[44] Importantly, the calculations correctly reproduce the nearly linear FeNO unit of $[Fe(S^tBu)_3(NO)]^-$ and the strongly bent one of the $[Fe(NS3)(NO)]^-$ anion, as well as the difference in Fe−N(O) distance between the two complexes (as shown in Scheme 2 and Table 4).

Figure 5a−d depict the MO energy level diagrams for the various FeNO complexes studied; however, in Figure 5a, we have approximated the $[Fe(S^tBu)_3(NO)]^-$ anion as $[Fe(SMe)_3(NO)]^-$. Assuming $C_{3v}$ symmetry for $[Fe(SMe)_3(NO)]^-$, with the $C_3$ axis identified with the *z* direction, we may rationalize the effective (Enemark−Feltham) d electron count of 7 in terms

(41) (a) Brown, C. A.; Pavovski, M. A.; Westre, T. E.; Zhang, Y.; Hedman, B.; Hodgson, K. O.; Solomon, E. I. *J. Am. Chem. Soc.* **1995**, *117*, 715−732. (b) Schenk, G.; Pau, M. Y. M.; Solomon, E. I. *J. Am. Chem. Soc.* **2004**, *126*, 505−515. (c) Rodriguez, J. H.; Xia, Y.-M.; Debrunner, P. G. *J. Am. Chem. Soc.* **1999**, *121*, 7846−7863. (d) Zhang, Y.; Oldfield, E. *J. Am. Chem. Soc.* **2004**, *126*, 9494−9495. (e) Zhang, Y.; Oldfield, E. *J. Phys. Chem. A* **2003**, *107*, 4147−4150. (f) Cheng, H.-Y.; Chang, S. *Int. J. Quant. Chem.* **2005**, *105*, 511−517.

(42) We have also studied the performance of additional functionals, including hybrid functionals, for the various molecules examined. The results do not reveal major differences among the different functionals examined; details of these investigations will be reported in a separate paper in the near future.

(43) For a recent discussion of the issue of pure versus hybrid functionals, see: Ghosh, A. *J. Biol. Inorg. Chem.* **2006**, *11*, 671−673.

(44) Conradie, J.; Ghosh, A. *Inorg. Chem.* **2006**, *45*, 4902−4909.

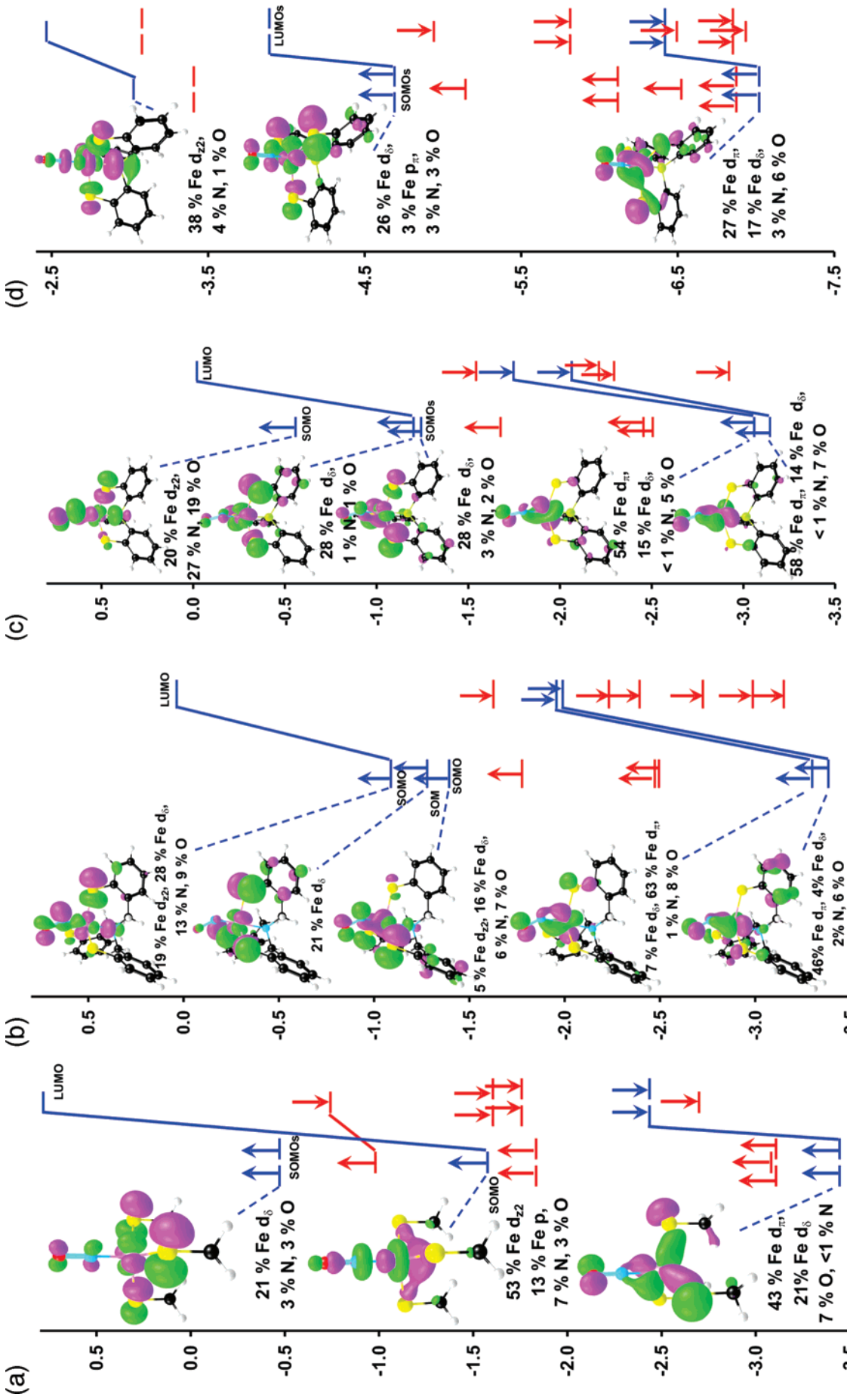


***Figure 5.*** PW91/TZP MO energy level (eV) diagrams for (a) $[Fe(SMe)_3(NO)]^-$, (b) $[Fe(NS3)(NO)]^-$, (c) $[Fe(PS3)(NO)]^-$, and (d) [Fe(PS3)(NO)]. MOs with substantial metal d character are indicated in blue, whereas MOs concentrated largely on the supporting thiolate ligands are indicated in red.

***Scheme 2***

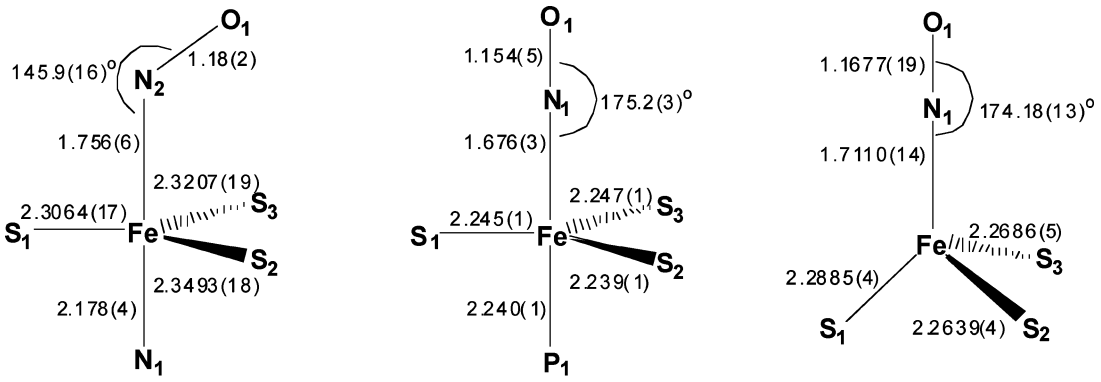


[Fe(NS3)(NO)]$^-$ (**1**) {FeNO}$^7$ | [Fe(PS3*)(NO)] (**2**) {FeNO}$^6$ | [Fe(S$^t$Bu)$_3$(NO)]$^-$ {FeNO}$^7$

of a $d_{xz}^2d_{yz}^2d_{z^2}^1d_{xy}^1d_{x^2-y^2}^1$ or, equivalently, a $d_\pi^2d_\pi'^2d_\sigma^1d_\delta^1d_\delta'^1$ orbital occupancy. Although these effective $d^7$ descriptions may suggest an Fe(I) oxidation state, note that the $d_{xz}$- and $d_{yz}$- (or $d_\pi$-) based MOs are really better described as $d_{xz}-\pi^*_{xz}$ and $d_{yz}-\pi^*_{yz}$ bonding combinations, with comparable Fe 3d and NO $\pi^*$ contributions. Indeed, Figures 3 and 4 reveal that the minority-spin $\pi^*$ electrons are actually spatially polarized toward the NO ligands, conferring on them an excess minority spin density. In other words, the NO ligands exhibit a certain $NO^-$ character, with a triplet-$O_2$-like spin density profile. However, both $Fe^I-NO^+$ and $Fe^{III}-NO^-$ are limiting case descriptions, and in view of the roughly even Fe 3d and NO $\pi^*$ contributions to the $\pi^*$ MOs, the real electronic structure seems best viewed as approximately halfway between these two limiting descriptions.[45]

Although the [Fe(NS3)(NO)]$^-$ anion deviates from exact threefold symmetry because of the bent FeNO unit, the electronic structure (Figure 5b) is qualitatively very similar to that described above. An exception is that the $d_\sigma/d_\pi$ distinction is lost, and therefore some of the majority spin density associated with the $d_{z^2}$ orbital now delocalizes into one of the $\pi^*$ orbitals of the NO group. As a result, as shown in Figure 4, the NO of [Fe(NS3)(NO)]$^-$ carries a smaller net minority spin population relative to the [Fe(S$^t$Bu)$_3$(NO)]$^-$ anion.

We can now return to a discussion of the FeNO angles. Why is the FeNO unit essentially linear in [Fe(S$^t$Bu)$_3$(NO)]$^-$ but substantially bent in [Fe(NS3)(NO)]$^-$? The standard argument for FeNO bending, namely the one made for {FeNO}$^7$ heme–NO derivatives, is that the bending permits Fe($d_{z^2}$)–NO($\pi^*$) $\sigma$-bonding, which is symmetry-forbidden for a linear FeNO unit.[16,29] However, recent theoretical work in one of our laboratories[33] shows that the degree of bending of the FeNO unit is extremely sensitive to the Fe hybridization state or, more precisely, to the exact shape of the Fe $d_{z^2}$-based MO. As may be seen from Figure 5a, the Fe $d_{z^2}$-based MO of the pseudotetrahedral $C_{3v}$ [Fe(SMe)$_3$(NO)]$^-$ complex has a distinctly unsymmetrical shape characterized by a shrunken top lobe that protrudes only slightly in the direction of the NO and a swollen bottom lobe. More precisely, the unusual shape of this MO may be attributed to a very substantial 13% Fe $p_z$ character, compared to about 53% Fe $d_{z^2}$ character. In contrast, in the TBP [Fe(NS3)(NO)]$^-$ case, the Fe $d_{z^2}$ orbital juts out much further toward the NO ligand, as a result of the antibonding interaction involving the NS3 amine ligand. This subtle difference in orbital topology or hybridization implies that Fe($d_{z^2}$)–NO($\pi^*$) $\sigma$-bonding is less critical in the [Fe(S$^t$Bu)$_3$(NO)]$^-$ case, resulting in a linear FeNO unit, unlike in the [Fe(NS3)(NO)]$^-$ case.

The scope of the above MO arguments may transcend this particular study. Thus, we may generalize that TBP {FeNO}$^7$ complexes with apical nitrosyls should exhibit substantially bent FeNO units, whereas the {FeNO}$^7$ units in four-coordinate pseudotetrahedral complexes should be essentially linear. To illustrate, the [Fe(N(CH$_2$CH$_2$S)$_3$)(NO)]$^-$ anion exhibits an FeNO angle of 154.4(9)°,[25] which is somewhat larger but qualitatively similar to that in [Fe(NS3)(NO)]$^-$. In contrast, like [Fe(S$^t$Bu)$_3$(NO)]$^-$, a recently reported tetrahedral triscarboxylato {FeNO}$^7$ complex exhibits an essentially linear FeNO group.[46] Similarly, crystallographic analyses have revealed an essentially linear FeNO geometry for the unique mononitrosyl center within the Roussin's black salt anion, [Fe$_4$($\mu^3$-S)$_3$(NO)$_7$]$^-$,[47] for which DFT calculations suggest an overall ($S = {}^5/_2$ $Fe^{III}$)$_4$–($S = 1$ $NO^-$)$_7$ description.[48] However, as discussed below, these generalizations are preliminary, and steric and electronic perturbations may lead to exceptions.[49]

Despite our focus on large variations in FeNO angles, we need to emphasize that the FeNO groups of $S = {}^3/_2$ {FeNO}$^7$ complexes are extremely flexible toward angular deformation. This point is illustrated in Figure 6 by means of potential energy curves for FeNO bending. As mentioned above, FeNO bending is particularly facile when it takes place concurrently with Fe–N(NO) tilting. This idea was originally advanced in terms of a potential energy function for carbonylhemes[31] and was subse-

(45) In other words, the {FeNO}$^7$ complexes may be best viewed as $Fe^{II}NO^\bullet$, which is consistent with recent theoretical analyses of the electron density in related systems.[36c,d,j,k,41f] Critics of such studies point out that analyses involving partitioning of the electron density among the Fe, N, and O and other atoms are inherently arbitrary and tantamount to characterizing "the unknowable (i.e., the oxidation state) in terms of the unobservable (atomic charges)": Ghosh, A. *J. Inorg. Biochem.* **2005**, *99*, vi–viii. On the other hand, like the spin density profiles in this study, X-ray absorption edge energies favor an $Fe^{III}NO^-$ description for certain {FeNO}$^7$ systems.[41a,b] Although attempts to assign metal and NO oxidation states in NO complexes are sometimes thought to generate more heat than light, such a view may be unduly dismissive. The main source of the problem is that the concept of oxidation state is not precisely defined. Therefore, controversy can be avoided by carefully defining the criterion or metric used when discussing metal and NO oxidation states.

(46) Klein, D. P.; Young, V. G., Jr.; Tolman, W. B.; Que, L., Jr. *Inorg. Chem.* **2006**, *45*, 8006–8008.

(47) D'Addario, S.; Demartin, F.; Grossi, L.; Iapalucci, M. C.; Laschi, F.; Longoni, G.; Zanello, P. *Inorg. Chem.* **1993**, *32*, 1153–1160.

(48) Jaworska, M.; Stasicka, Z. *J. Mol. Struct.* **2006**, *785*, 68–75.

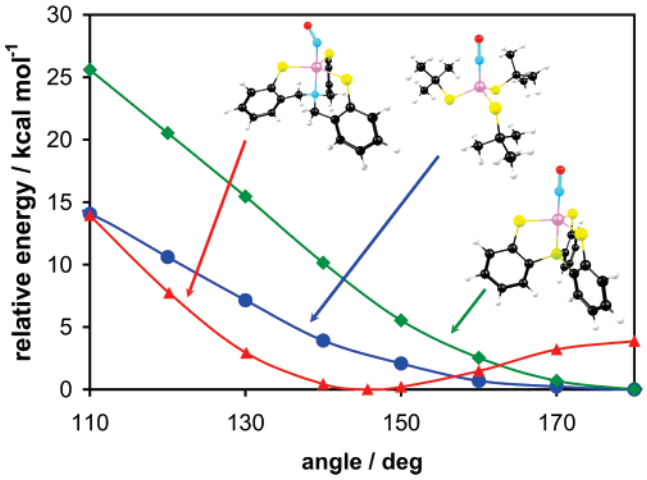


***Figure 6.*** PW91/TZP potential energy curves for $[Fe(NS3)(NO)]^-$ ($S = {}^3/_2$, in red) $[Fe(S^tBu)_3(NO)]^-$ ($S = {}^3/_2$, in blue) and $[Fe(PS3)(NO)]$ ($S = 1$, in green) as a function of the Fe−N−O angle, all other internal coordinates being optimized at each data point shown.

quently extended to other $\{MXO\}^6$ and $\{MXO\}^7$ systems.[33] The strong cooperativity of tilting and bending deformations can be easily understood in terms of MO arguments. Cooperative tilting and bending result in minimum disruption of metal−XO (X = C, N) $\pi$-backbonding, whereas FeN tilting in one direction and FeNO bending in the other direction strongly disrupt the backbonding and are therefore energetically very costly and hence never observed in crystal structures. Armed with this perspective, we can better appreciate the energy cost of FeNO bending in $[Fe(S^tBu)_3(NO)]^-$ by a substantial angle, for example, 30° from linearity. Figure 6 shows that the energy cost is barely a couple of kcal/mol. Indeed, very recently, the crystal structure of a second $\{FeNO\}^7$−tristhiolate complex, $[Fe(SPh)_3(NO)]^-$, has been reported, revealing a modestly bent FeNO angle of 164.6°.[50] Thus, the generalizations made above are not hard and fast rules, given the extreme softness of the bending potential.

A theoretical comparison of $[Fe(S^tBu)_3(NO)]^-$ and $[Fe(NS3)(NO)]^-$ would not be complete without some discussion of experimental observations on the relative stability of the two compounds. We have already mentioned that $[Fe(NS3)(NO)]^-$, in spite of having the longer Fe−N(O) bond, is a rather robust species with no tendency toward NO dissociation at room temperature. In contrast, all the known $\{FeNO\}^7$−tristhiolate complexes are highly photosensitive. Liaw and co-workers have emphasized that, whereas the $[Fe(SPh)_3(NO)]^-$ anion is extremely photosensitive, the ethyl analogue, $[Fe(SEt)_3(NO)]^-$, which they also synthesized, is only somewhat less so.[50] Because DFT is essentially a ground-state theory, the photochemical behavior of these compounds cannot be easily modeled theoretically. However, the MO energy level diagrams of $[Fe(SMe)_3(NO)]^-$ (Figure 5a) and of $[Fe(NS3)(NO)]^-$ (Figure 5b) provide a potential explanation for their different photostabilities. For both molecules, the LUMO is a $d_{z^2}$-based minority-spin MO, the unoccupied $\beta$ partner of the corresponding occupied α MO. However, as may be seen from Figure 5a,b, the $\beta$-HOMO−$\beta$-LUMO gaps are somewhat different for the two compounds: 1.5 eV for $[Fe(SMe)_3(NO)]^-$ vs 1.7 eV for $[Fe(NS3)(NO)]^-$. In addition, the topologies of the $d_{z^2}$-based MOs in the two complexes are also substantially different. Whereas in $[Fe(SMe)_3(NO)]^-$ this MO is antibonding with respect to the Fe−NO linkage, the corresponding MO in $[Fe(NS3)(NO)]^-$ is *bonding* across the same linkage, because of the bent FeNO geometry (see Figure 5a,b). Consequently, only for an $\{FeNO\}^7$−tristhiolate complex (as opposed to an NS3 complex) does the $\beta$-HOMO → $\beta$-LUMO transition, which is the lowest-energy non-spin-flip transition, result in a dissociative $d_{z^2}$ state. It appears that the HOMO−LUMO gap and the LUMO topology, in concert, result in the extreme light sensitivity of one complex, versus the relative stability of the other.

**A Broader Perspective of d/p Hybridization Effects.** In the discussion above, we attributed the difference in FeNO conformation between $[Fe(S^tBu)_3(NO)]^-$ and $[Fe(NS3)(NO)]^-$ to a difference in d orbital hybridization (i.e., Fe $p_z$ admixture in the case of the former complex) as a result of different stereochemistries. Although special, such effects are by no means unique and therefore deserve a certain contextualization. Variations in FeNO angles resulting from different Fe hybridizations are also known for low-spin $S = {}^1/_2$ $\{FeNO\}^7$ systems. For example, although $\{FeNO\}^7$ heme−NO systems invariably exhibit bent FeNO units, the TBP [Fe(5,5-tropocoronand)(NO)] complex, which has an equatorial (as opposed to an apical) NO,[51,52] and the square-pyramidal $[Fe(CN)_4(NO)]^{2-}$ anion exhibit linear $\{FeNO\}^7$ units.[53] As in this study, the exact shape of the $d_\sigma$-based MOs of these low-spin $\{FeNO\}^7$ complexes appears to be the critical factor controlling FeNO bending.

Adopting an even broader perspective, we may connect some of the above electronic-structural findings to an entirely different area of inorganic chemistry, viz. recent findings on low-coordinate middle and late transition metal imido complexes.[54] A relatively low-energy, unsymmetrical $d_{z^2}$ orbital, not unlike the one described above for $[Fe(S^tBu)_3(NO)]^-$, is also found in pseudotetrahedral iron and cobalt imido complexes.[55] Thus, for example, $Fe^{III}$ and $Co^{III}$ imido complexes with trisphosphine supporting ligands exhibit low-spin $d_\delta{}^2 d_\delta{}'^2 d_{z^2}{}^1$ and $d_\delta{}^2 d_\delta{}'^2 d_{z^2}{}^2$ configurations, respectively.[54] In other words, the $\sigma$-antibonding $d_{z^2}$ orbital is preferentially occupied, as opposed to the $d_\pi$ orbitals. The reason is that for these complexes, as in the case of the $[Fe(S^tBu)_3(NO)]^-$ anion, the $d_{z^2}$-based MO has considerable metal $p_z$ character, resulting in surprisingly muted $\sigma$-antibonding interactions involving the imido ligand.[55] Similar (although not exactly the same) considerations also explain the stability of middle and late transition metal−imido complexes with $\beta$-diketiminato (nacnac) supporting ligands.[56]

**Theoretical Description of [Fe(PS3)(NO)].** Figure 7 depicts PW91 geometries and spin density profiles of the three

(49) Borovik and coworkers have reported a series of three $S = {}^3/_2$ TBP $\{FeNO\}^7$ triamidoamine complexes with increasingly sterically hindered R groups on the amidato nitrogens.[23] For R = 3,5-dimethylphenyl, cyclopentyl, and isopropyl, the FeNO angles were found to be 160.3(2)°, 172.7(4)°, and 178.2(5)°, respectively. The increasing linearity of the FeNO angles along this series should not be viewed as a failure of our generalizations, but rather as a result of the increasingly sterically hindered nature of the R groups.

(50) Lu, T.-T.; Chiou, S.-J.; Chen, C.-Y.; Liaw, W.-F. *Inorg. Chem.* **2006**, *45*, 8799−8806.

(51) Franz, K. J.; Lippard, S. J. *J. Am. Chem. Soc.* **1999**, *121*, 10504−10512. Addition/Correction: *J. Am. Chem. Soc.* **2001**, *123*, 1266−1266.

(52) Tangen, E.; Conradie, J.; Ghosh, A. *Inorg. Chem.* **2005**, *44*, 8699−8706.

(53) Conradie, J.; Ghosh, A. *J. Inorg. Biochem.* **2006**, *100*, 2069−2073.

(54) Mehn, M. P.; Peters, J. C. *J. Inorg. Biochem.* **2006**, *100*, 634−643 and references therein.

(55) Tangen, E.; Conradie, J.; Ghosh, A. *J. Chem. Theory Comput.* **2007**, *3*, 448−457.

(56) Conradie, J.; Ghosh, A. *J. Chem. Theory Comput.* **2007**, *3*, 689−702.

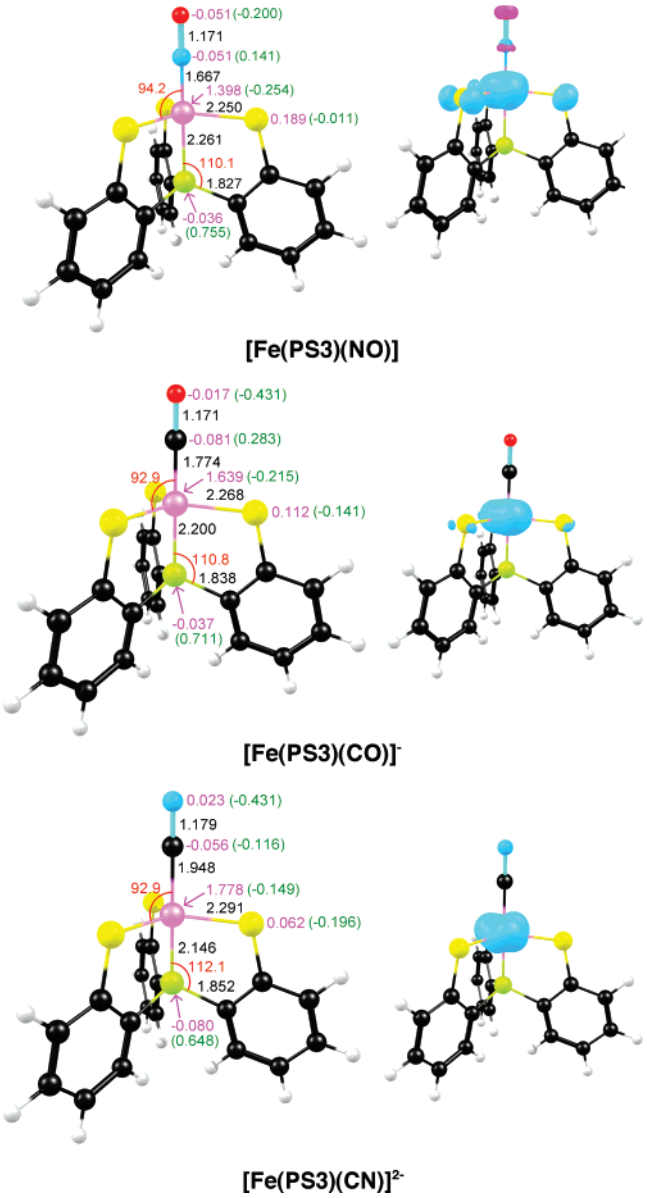


***Figure 7.*** Selected PW91/TZP results for the three $C_{3v}$ $S = 1$ Fe(PS3)(XY) complexes studied. Left: Distances (Å, in black), angles (deg, in red), Mulliken spin populations (in magenta), and charges (in green). Right: Molecular spin density plots; majority and minority spin densities are indicated in cyan and magenta, respectively.

isoelectronic $S = 1$ [Fe(PS3)(XY)] species, where XY = CO, NO, and CN.[17a,34] Careful testing showed that the three complexes exhibit exact $C_{3v}$ symmetry. For [Fe(PS3)(NO)], the PW91 Fe−N(NO) distance is 1.667 Å, which is about the same as that in $[Fe(S^tBu)_3(NO)]^-$ (1.681 Å) but significantly shorter than that in $[Fe(NS3)(NO)]^-$ (1.726 Å). These results imply that, for similar TBP coordination geometries, Fe−NO backbonding is much stronger in the $\{FeNO\}^6$ complex than in related $\{FeNO\}^7$ complexes. Stronger $\pi$-backdonation also explains the stiffer potential associated with FeNO bending in [Fe(PS3)(NO)] than in $\{FeNO\}^7$ systems studied (see Figure 6). For the $S = 1$ PS3 complexes, note also that the optimized Fe−X(XY) distances lengthen in the order [Fe(PS3*)(NO)] < $[Fe(PS3^*)(CO)]^-$ < $[Fe(PS3)(CN)]^{2-}$, i.e., with decreasing $\pi$-acceptor ability of the XY ligand, whereas the Fe−P distances vary in the reverse order, namely [Fe(PS3*)(NO)] > $[Fe(PS3^*)(CO)]^-$ > $[Fe(PS3)(CN)]^{2-}$. It appears that metal−phosphorus bonding increases with and compensates for decreasing Fe-to-XY $\pi$-donation. These calculated structural trends nicely parallel those observed experimentally,[17a,34] as described above.

The effective $d^6$ electronic configuration of these $S = 1$ complexes may be described as $d_{xz}^2 d_{yz}^2 d_{xy}^1 d_{x^2-y^2}^1$ or, equivalently, as $d_\pi^2 d_{\pi'}^2 d_\delta^1 d_{\delta'}^1$, which results in a flattened (oblate) spheroid of majority spin density at the iron center, as shown in Figure 7. Compared with $[Fe(S^tBu)_3(NO)]^-$, the NO group in [Fe(PS3)(NO)] harbors a significantly smaller quantity of minority spin density. Besides, [Fe(PS3)(NO)] exhibits substantially higher N and O Mulliken charges than the $\{FeNO\}^7$ systems studied, which might be viewed as indicative of an $Fe^{II}-NO^+$ description.

The PS3* ligand seems to be unique in terms of its ability to stabilize the $S = 1$ $\{FeNO\}^6$ state. Neither simple trithiolate coordination nor the NS3 ligand results in an isolable $\{FeNO\}^6$ complex. Similarly, electrochemical oxidation of a triamidoamine ($NN_3$) $\{FeNO\}^7$ complex resulted only in an unstable, presumably $\{FeNO\}^6$ intermediate. Our calculations nicely reflect this experimental scenario. According to the energy level diagrams shown in Figure 5, the $d_{z^2}$-based SOMO of [Fe(PS3)(NO)]$^-$ has a considerably higher orbital energy than the analogous MO in both $[Fe(S^tBu)_3(NO)]^-$ and $[Fe(NS3)(NO)]^-$, as a result of the very strong $Fe(d_{z^2})-P(sp^3)$ antibonding interaction. In the same vein, the calculated PW91/TZP adiabatic ionization potentials (IPs) of $[Fe(S^tBu)_3(NO)]^-$, $[Fe(NS3)(NO)]^-$, and [Fe(PS3)(NO)]$^-$ are 2.60, 2.55, and 2.06 eV, respectively. We have checked that this trend in the IPs remains unchanged for a wide range of common exchange-correlation functionals.

## Conclusion

Our main findings may be enumerated as follows.

1. We have described the synthesis and structural characterization of two new nonheme iron−thiolate−NO complexes, the $S = {}^3/_2$ $[Fe(NS3)(NO)]^-$ anion and the unique $S = 1$ $\{FeNO\}^6$-[Fe(PS3*)(NO)] complex.

2. The compounds exhibit interesting structural features. Like the $S = 0$ $\{FeNO\}^6$ porphyrins, $S = 1$ [Fe(PS3*)(NO)] displays an exceptionally short Fe−N(NO) distance of about 1.67 Å. In addition, there are large variations in the FeP distance for the $S = 1$ isoelectronic series [Fe(PS3)(XY)] (XY = NO, CO, $CN^-$), which decreases with decreasing $\pi$-acceptor strength of the diatomic ligand.

3. The electrochemical properties of $[Fe(NS3)(NO)]^-$ and of [Fe(PS3*)(NO)] exhibit marked differences. The former irreversibly oxidizes with NO loss at a potential of +0.394 V, while the latter exhibits a reversible $\{FeNO\}^6/\{FeNO\}^7$ couple at −0.127 V, both potentials being vs SCE.

4. Consistent with the electrochemical picture, DFT (PW91/TZP) calculations predict gas-phase adiabatic ionization potentials of 2.60, 2.55, and 2.06 eV for $[Fe(S^tBu)_3(NO)]^-$, $[Fe(NS3)(NO)]^-$, and [Fe(PS3)(NO)]$^-$, respectively.

5. DFT calculations underscore the importance of *trans* influences in determining key properties of the NO complexes studied. Thus, the strong *trans* influence of the phosphine (which destabilizes the $d_{z^2}$ orbital) is the key factor that stabilizes the $\{FeNO\}^6$ oxidation state of the [Fe(PS3)(NO)] complex.

6. An antibonding interaction involving the metal $d_{z^2}$ orbital and the amine lone pair, in effect, the *trans* influence of the amine ligand, appears to be the key determinant of the bent

FeNO geometry of $[Fe(NS3)(NO)]^-$. In contrast, the lack of a *trans* ligand in $[Fe(S^tBu)_3(NO)]^-$ results in an Fe-$p_z$-admixed, stereochemically inactive $d_{z^2}$ orbital, resulting, in turn, in an unusual, linear FeNO unit.

7. An examination of the literature suggests that this last MO argument (i.e., conclusion no. 6) may transcend the specific complexes studied here. Thus, we predict that $S = {}^3/_2$ trigonal-bipyramidal $\{FeNO\}^7$ complexes with apical NOs should in general exhibit substantially bent FeNO groups, whereas tetrahedral $S = {}^3/_2$ $\{FeNO\}^7$ complexes should exhibit nearly linear FeNO groups.

8. Finally, we have pointed out that metal-$p_z$-admixed, stereochemically inactive $d_{z^2}$ orbitals are also found in low-coordinate middle and late transition metal−imido complexes. Indeed, such orbitals may be a common feature of the bonding in many low-coordinate complexes.

## Experimental Section

**Syntheses.** All reactions were carried out under a nitrogen atmosphere using Schlenk techniques.

**$[Me_4N][Fe(NS3)(NO)]$ (1).** The pale yellow $Li[Fe(N(CH_2\text{-}o\text{-}C_6H_4S)_3)]$ salt was generated in methanol by the reaction of $Li_3(N(CH_2\text{-}o\text{-}C_6H_4S)_3)$ (0.44 g, 1.01 mmol) and $FeCl_2{\cdot}4H_2O$ (0.199 g, 1.00 mmol). NO was bubbled into the reaction mixture resulting in the formation of a small amount of fine pale chocolate-brown solid dispersed in a deep mahogany solution. The side-product was removed by filtration, and the filtrate was concentrated and layered with 10 mL of a solution of $Me_4NBr$ (0.155 g, 1.01 mmol) in methanol. After 24 h at room temperature, the product crystallized as brown cubes. The product can be recrystallized from DMF/EtOH with a yield of 0.25 g (47%). IR (Nujol): $\nu_{NO} = 1639\ cm^{-1}$. Anal. Calcd (Found) for $[Me_4N][Fe(NS3)(NO)]$, $C_{25}H_{30}FeN_3OS_3$: C, 55.55 (55.83); H, 5.59 (5.45); N, 7.77 (7.44). $\mu_{eff} = 3.76\ \mu_B$ at room temperature.

**[Fe(PS3*)(NO)] (2):** The reaction of $FeCl_2{\cdot}4H_2O$ (0.034 g, 0.17 mmol) with 0.17 mmol of deprotonated tris(3-phenyl-2-thiophenyl)-phosphine, $Li_3[PS3^*]$, in 15 mL of MeOH generates a green solution. Upon the addition of NO, the solution became dark blue from which a microcrystalline solid readily precipitated. The solid was filtered and recrystallized from dichloromethane and hexane to give 0.101 g (89% yield) of product. $^1H$ NMR (DMSO-$d^6$): $\delta$ −45.33 (3H), 2.60 (3H), 6.65 (3H), 8.50 (6H), 9.49 (6H), 24.03 (3H). UV−vis (DMF), $\lambda_{max}$ (nm) ($\epsilon_M$): 552 ($2.12 \times 10^3$), 856 ($1.93 \times 10^3$). IR (Nujol): $\nu_{NO} = 1807\ cm^{-1}$. Anal. Calcd (Found) for [Fe(PS3*)(NO)], $C_{36}H_{24}FeNOPS_3$: C, 64.57 (65.21); H, 3.61 (3.31); N, 2.09 (2.24). $\mu_{eff} = 2.70\ \mu_B$ at RT.

**Cyclic Voltammetry**. All cyclic voltammetry experiments were carried out in DMF with 1 M $[n\text{-}Bu_4N][BF_4]$, using a Pt working electrode and a saturated calomel electrode as a reference electrode.

**X-ray Crystal Structure Determinations.** Unit cell determination and data collection were done at room temperature using an Enraf-Nonius CAD4 diffractometer with Mo radiation.

**$[Me_4N][Fe(NS3)(NO)]{\cdot}MeOH$:** Brown cubic crystals were grown from the original reaction mixture. A crystal (0.36 mm × 0.32 mm × 0.26 mm), obtained from the mother liquor, was immersed in mineral oil. Monoclinic, space group $P2_1/c$, $a = 16.748(2)$ Å, $b = 10.335(2)$ Å, $c = 17.844$ Å(2), $\beta = 114.051(10)°$, $V = 2821$ Å$^3$, $Z = 4$). The structure was solved and refined using the SHELX programs. Data collection and processing produced 2138 reflections (4877 total). Least-squares refinement vs $F^2$ completed the structure (R1 = 0.063, wR2 = 0.130) for observed data and (R1 = 0.1294, wR2 = 0.149) for all data.

**[Fe(PS3*)(NO)]:** Crystals were grown by vapor diffusion from methylene chloride and hexane. A black crystal measuring 0.3 × 0.4 × 0.4 mm$^3$ was mounted in a glass capillary and sealed by epoxy resin. The structure was solved under the orthorhombic primitive crystal system (space group *Pbca*), with the following unit cell: $a = 17.590(1)$ Å, $b = 17.765(1)$ Å, $c = 19.847(2)$ Å, $V = 6201.9(7)$ Å$^3$. A DIFABS empirical absorption correction was applied, and the structure was refined versus $F$ using the Texsan series of programs to a final $R(R_w)$ of 0.041(0.024).

**DFT Calculations.** In general, all calculations were carried out using the PW91[57] generalized gradient approximation (GGA) for both exchange and correlation, triple-$\zeta$ plus polarization Slater-type orbital basis sets, and a fine mesh for numerical integration of matrix elements, all as implemented in the ADF 2005[58] program system. As a check on the performance of the PW91 functional, the OLYP[59] GGA was also used for several calculations. In general, the PW91 GGA favors a more covalent, spin-paired description for transition metal−ligand interactions, compared to OLYP.[56] In this study, however, both GGAs yield ressonably similar results (geometries, spin densities, and energetics).

**Acknowledgment.** This work was supported by the Research Council of Norway (A.G.), the National Research Fund of the Republic of South Africa (J.C.), the U.S. National Institutes of Health (GM58000 to S.A.K.), the U.S. National Science Foundation (CHE-0611944 to S.J.L.). T.C.H. acknowledges the National Institutes of Health for a postdoctoral fellowship (1 F32 GM075684-01). Lu Gan is thanked for experimental assistance.

**Supporting Information Available:** Tables of crystal data and structure refinement for **1**, crystallographic data for **2**, and Cartesian coordinates for **1**−**2** (PDF); X-ray crystallographic data for **1** and **2** (CIF). This material is available free of charge via the Internet at http://pubs.acs.org.

JA0719982

(57) (a) Perdew, J. P.; Chevary, J. A.; Vosko, S. H.; Jackson, K. A.; Pederson, M. R.; Singh, D. J.; Fiolhais, C. *Phys. Rev. B* **1992**, *46*, 6671−6687. (b) Perdew, J. P.; Chevary, J. A.; Vosko, S. H.; Jackson, K. A.; Pederson, M. R.; Singh, D. J.; Fiolhais, C. *Phys. Rev. B* **1993**, *48*, 4978−4978.
(58) Velde, G. T.; Bickelhaupt, F. M.; Baerends, E. J.; Guerra, C. F.; Van Gisbergen, S. J. A.; Snijders, J. G.; Ziegler, T. *J. Comput. Chem.* **2001**, *22*, 2001.
(59) Handy, N. C.; Cohen, A. J. *Mol. Phys.* **2001**, *99*, 403−412.